



# Experimental and numerical analysis of air temperature uniformity in occupied zone under stratum ventilation for heating mode

Junmeng Lyu <sup>a,1</sup>, Xuan Feng <sup>a,1</sup>, Yong Cheng <sup>a,b,c</sup>, Chunhui Liao <sup>d,\*</sup>

<sup>a</sup> School of Civil Engineering, Chongqing University, Chongqing, China

<sup>b</sup> Joint International Research Laboratory of Green Buildings and Built Environments, Ministry of Education, Chongqing University, Chongqing, China

<sup>c</sup> National Centre for International Research of Low-carbon and Green Buildings, Ministry of Science & Technology, Chongqing University, Chongqing, China

<sup>d</sup> Institute for Health and Environment, Chongqing University of Science and Technology, Chongqing, China

## ARTICLE INFO

### Keywords:

Stratum ventilation

Heating

Air temperature distribution

Grey relational analysis

Supply air parameters

## ABSTRACT

In warm air heating systems, a good indoor air temperature distribution can provide a comfortable indoor environment and reduce energy consumption. Few studies were conducted for the uniformity of air temperature distributions under stratum ventilation (SV) for heating. In this study, the horizontal and vertical air temperature uniformities in an occupied zone were evaluated under SV heating mode. Different indoor thermal environments were created using both experiments and computational fluid dynamics (CFD) simulations. Results showed that the horizontal air temperature uniformity is generally inferior to the vertical direction. Based on the experimental and simulation cases, the maximum horizontal and vertical air temperature gradient is 3.46 °C/m and 2.44 °C/m, respectively. The uniformity of the air temperature distribution can be significantly affected by supply air parameters. The maximum extremum air temperature difference is 6.26 °C at the height of 0.6 m. However, it can be reduced to less than 0.62 °C by varying the supply air velocity, temperature and angle. Appropriate supply air parameters can provide an energy utilization coefficient (EUC) higher than one, showing the potentials of energy saving. A grey relational analysis revealed that the relational degree of the supply air velocity and temperature on the air temperature uniformity is relatively high, followed by the outdoor temperature and then supply vane angle. The results derived from this study can contribute to better understand the characteristics of indoor air temperature distribution under SV heating mode.

## 1. Introduction

In the present society, most individuals spend 80%–90% of their lives indoors. Therefore, sufficient fresh air, appropriate air temperatures and air velocities are generally required for indoor environments [1]. The application of heating, ventilation, and air conditioning (HVAC) systems in buildings is essential for satisfying this requirement. Because the energy consumption of an HVAC system is the main component of a building's total energy consumption [2,3], a rapid increase in the former would cause a significant increase in the total building energy consumption. Consequently, the environmental pollution caused by the energy consumption would become increasingly severe [4]. Therefore, the provision of a healthy and comfortable indoor environment is related to the quality of life and work efficiency, and to the global energy consumption and environmental pollution [5–9].

Warm air heating is a common indoor environment conditioning method used in winter. The air distribution methods include mixing ventilation, wall confluent jet ventilation, impinging jet ventilation, and underfloor air distribution [9–12]. Mixing ventilation is widely used in traditional air distribution owing to its advantages with regard to convenient installation and year-round operation. However, because both air inlets and outlets are typically installed near the ceiling, it is difficult to send warm air into the occupied zone owing to the effects of thermal buoyancy. This causes a lower air temperature in the occupied zone and higher air temperature in the upper zone of the room. This, in turn, can easily result in excessive air temperature stratification and/or short circuiting between the inlets and outlets [12]. Excessive air temperature stratification would develop a thermal discomfort condition referred to as “warm head and/or cold feet.” Moreover, the higher air temperatures in the upper zone comprise an efficient usage of the warm supply airflow, which increases the heating energy consumption

\* Corresponding author.

E-mail address: [aoxue007@163.com](mailto:aoxue007@163.com) (C. Liao).

<sup>1</sup> These two authors contributed equally and should be considered as co-first authors.

<b>Nomenclature</b>	
$A_s$	supply vane angle, °
$T_s$	supply air temperature, °C
$V_s$	supply air velocity, m/s
$T_w$	exterior wall temperature, °C
$\varepsilon_{0i}$	grey relational coefficient
$\rho$	distinguishing coefficient
$\gamma_{0i}$	grey relational grade
$N$	number of simulation groups
$T_{im}$	local air temperature at i m, °C
$T_{ave\_max}$	maximum of the average temperature at each height, °C
$T_{ave\_min}$	minimum of the average temperature at each height, °C
$T_{im\_ave}$	surface average temperature at height of i m, °C
$\Delta T_{ave}$	average value of vertical air temperature differences, °C
$SD_i$	standard deviation of local air temperature at i m
$SD_v$	standard deviation of the plane average temperature
$SD_h$	among 0.1 m, 0.6 m, 1.1 m, and 1.7 m average of standard deviation of local air temperature at each height
$\Delta T_h$	average maximum temperature gradient in each plane in the horizontal direction, °C/m
$\Delta T_v$	average maximum temperature gradient in the vertical direction, °C/m
<b>Abbreviations</b>	
GRA	grey relational analysis
GTS	grey system theory
GRG	grey relational grade
SD	standard deviation
VTD	vertical air temperature difference
DO	discrete ordinates
EUC	energy utilization coefficient

[13–15]. Wall confluent jet ventilation causes multiple jets to flow through an air supply device and then to move along the wall and merge. These ultimately impact the floor and send the air into the occupied zone. In winter, to reduce the vertical air temperature difference between the head and ankle levels in the occupied zone, a high-speed jet (generally higher than 7 m/s) is used to ensure that warm air can be sent to the near-ground surface of the occupied zone. Although such a system can effectively solve the problem of air temperature stratification, the energy consumption is relatively high [10]. The underfloor air distribution and impinging jet ventilation have become popular in recent decades. This is because these can solve the problem of excessive air temperature stratification whilst maintaining low energy consumption and thereby, yield a comfortable indoor heating environment in winter [16–20]. To summarize, these studies on the various air distribution methods for warm air heating were focused on the exploration of the characteristics of the corresponding indoor temperature distributions. Their aims were to provide theoretical support for improving the indoor thermal environment under warm air heating mode.

Stratum ventilation (SV) is a novel air distribution method. The conditioned air is supplied directly to the occupied zone through air diffusers installed at the height of 1.3 m above floor on the side walls [21]. It can provide a thermally comfortable indoor environment, with comfortable room air temperatures of up to approximately 27 °C for the cooling mode [21,22]. In winter, SV is a feasible air distribution for supplying warm air. Although extensive studies have addressed the SV cooling mode, few studies have been conducted on SV for the heating mode. This is owing to its short development history. Cheng et al. [23] focused on the flow characteristics of airflow, analyzed the turbulence characteristics of a warm airflow under SV heating, and evaluated local thermal discomfort. Liang et al. [24] proposed optimal parameter ranges for the supply air temperature and velocity under an SV heating mode using a Pareto-based multiple objective particle swarm optimization and cluster analysis. Kong et al. [25] observed that SV could save 25% of the energy required for indoor thermal comfort as compared with mixing ventilation. Zhang et al. explored the influences of the supply air parameters on the system performance under the SV heating mode [26]. Furthermore, they discussed a design method for the supply air parameters based on the optimization of thermal comfort, energy utilization efficiency, and CO<sub>2</sub> removal efficiency [27]. They observed that the effect of the supply air parameters was more complex in the heating mode. This is because warm airflow is significantly affected by thermal buoyancy. In general, for the heating mode, the supply vane angle of an SV system needs to be adjusted downward to cause the warm air to flow into the occupied zone. Furthermore, the supply air velocity may need to be higher than 1 m/s to obtain a sufficiently high initial momentum and

weaken the adverse effect of thermal buoyancy. In addition, when the supply air temperature is excessively high, the indoor air temperature cannot satisfy the comfort temperature range of 18–24 °C recommended by American Society of Heating, Refrigerating, and Air-Conditioning Engineers (ASHRAE)-55 [28]. Moreover, the effect of the thermal buoyancy is strengthened further, which hinders the transport of the warm air into the occupied zone. The above studies on the SV heating mode mainly focused on indoor thermal comfort and system performance optimization. Meanwhile, relatively few studies have evaluated the uniformity of indoor air temperature distribution. In particular, horizontal air temperature distribution is mentioned infrequently. However, for warm air heating, under the effect of thermal buoyancy, indoor air temperature stratification is more likely to occur, and the indoor air temperature distribution is more complex. Thus, air temperature uniformity is highly important. Because the air temperature distribution is closely related to energy consumption and occupants' comfort, it is particularly important to clarify the characteristics of indoor air temperature distribution under the specific air distribution method used for warm air heating. Nevertheless, SV uses a non-isothermal free jet. The jet energy decays along the jet direction, and the volume of the air entrainment varies. These result in significant air temperature variations along the jet direction [23]. Therefore, the horizontal air temperature distribution under SV may be non-uniform. A study of the temperature distribution can enable a more comprehensive understanding of the temperature distribution characteristics of SV while heating a room. Based on the research results, the optimization of air distribution can be explored further to achieve good indoor thermal comfort on the basis of low energy-consumption operation of the SV heating system. This would contribute to the reduction of building energy consumption.

Considering the above, this study was aimed at evaluating the uniformity of the horizontal and vertical air temperatures in an occupied zone under an SV heating mode, according to the common air supply parameters and outdoor weather conditions. Both experiments and computational fluid dynamics (CFD) simulations were used to comprehensively analyze the air temperature uniformity characteristics of the occupied zone in different indoor thermal environments. Meanwhile, based on the standard deviation (SD) of the horizontal air temperature and the vertical air temperature difference, the relational grades of the supply air parameters including supply vane angle, supply air temperature, supply air velocity and exterior wall temperature on the air temperature uniformity were obtained using grey relational analysis (GRA). The research results are effective for future optimizations and practical applications of SV heating systems.

## 2. Research methodology

### 2.1. Experiments

#### 2.1.1. Test chamber

The experiments were conducted in a test chamber at Chongqing University during winter. As shown in Fig. 1, a chamber was constructed to simulate a typical office. It had dimensions of 5.85 m (length)  $\times$  5.06 m (width)  $\times$  2.55 m (height). All the walls were interior walls. A window was installed on the right wall (see Fig. 1), and the window-to-wall ratio was 0.26. An SV heating system was used in this test chamber. Three double-deflection grille diffusers (0.18 m  $\times$  0.18 m) were installed at a height of 1.3 m on the front wall. Three air outlets (0.18 m  $\times$  0.18 m) were installed at a height of 0.4 m above the floor and located below the supply air diffusers. The occupants were simulated using rectangular thermal manikins with dimensions of 0.4 m (length)  $\times$  0.25 m (width)  $\times$  1.2 m (height). Each manikin was heated using a 100 W light bulb. Previous studies had experimentally verified that it is adequate to use a rectangular thermal manikin for simulating the interactions between an occupant and the indoor thermal environment [29] under SV. Six 23 W ceiling lamps were used for illumination. A full fresh air system was used in the experiments.

Information on the measurement tools is summarized in Table 1. The measurement range of air velocity was 0.05–3.00 m/s. Furthermore, the measurement error was  $\pm 0.03$  m/s in the range of 0.05–1.00 m/s and  $\pm 3\%$  of readings in the range of 1.00–3.00 m/s. The measurement range of air temperature was 10–40 °C, and the measurement error was  $\pm 0.2$  °C. The measurement range for the thermocouple system (used to measure the wall surface temperatures) was –20–80 °C, and the measurement error was  $\pm 0.3$  °C. During the experiments, the indoor relative humidity was approximately 47%.

#### 2.1.2. Test procedure

All the measurements were conducted under steady conditions. Ten sampling lines were set up to fully analyze the influences of the different parameters on the indoor air temperature distribution. The sampling lines L1, L2, L5, L6 and L9 were arranged along the direction of the jet flow; L10 was arranged in the non-jet flow area; and L3, L4, L7, and L8 were arranged close to the thermal manikin. SWEMA omnidirectional anemometer systems were used to measure local air velocity and air temperature along the ten sampling lines (L1–L10) at five heights above the floor: 0.1 m, 0.6 m, 1.1 m, 1.7 m, and 2.4 m (Fig. 2). The measurement time for each sampling line was 12 min. The sampling

**Table 1**  
Information on measurement tools.

Measured parameter	Tool	Measurement error
Air temperature	SWEMA omnidirectional anemometer system	$\pm 0.2$ °C between 10 and 40 °C
Air velocity	SWEMA omnidirectional anemometer system	$\pm 0.03$ m/s between 0.05 and 1.00 m/s $\pm 3\%$ of reading between 1.00 and 3.00 m/s
Wall surface temperature	Thermocouple system	$\pm 0.3$ °C between –20 and 80 °C

frequency of the SWEMA system was 1 Hz. After the measurement of a sampling line was completed, the measuring rod was moved to the next sampling line after an interval of 10 min (to ensure the stability of the indoor flow). Then, the local air temperature and velocity were measured at all the measuring points along these sampling lines.

The room air temperature was measured by a thermocouple in the center of the occupied zone (0.2 m above the center of the table). In this study, the supply air vane angle was fixed at 30° (downward) in all the experimental conditions. This was done to oppose the effect of thermal buoyancy. Studies have shown that the supply air velocity, which is generally higher than 1 m/s, can inhibit the upward movement of warm air [30]. Thus, the measured air velocities were set to 0.92 m/s and 1.42 m/s, respectively. In general, thermal buoyancy is moderate when the supply air temperature is 24–26 °C, and the air can be transported to the occupants for heating [26]. Therefore, the air supply temperatures were set to 24 °C and 26 °C in this experiment. After the pre-experiments, the room air temperature was controlled at 18–24 °C, as specified by ASHRAE-55. Information on the three experimental cases is presented in Table 2.

### 2.2. Computational fluid dynamics (CFD) simulations

#### 2.2.1. Numerical modeling and boundary conditions

Experimental measurements and CFD simulations are two popular methods for studying indoor environments with various air distributions. Although experimental measurements are more objective, these are more time-consuming and expensive. Previous studies have shown that CFD simulations (after validated by experimental measurements) can reliably predict indoor air flows and indoor air temperatures. CFD simulations are widely used because of their low costs [31–36]. In the simulation studies, the right wall was set as the exterior wall so as to consider the influence of the outdoor environment on the indoor thermal environment, as shown by the blue wall in Fig. 1. The physical model used in the experiment was constructed in the CFD simulations. Airpak 3.0.16 was used to construct the physical model and generate the mesh. The ANSYS Fluent program was used to compute the airflows and air temperature distributions in the test chamber [37].

The inlets and outlets in the CFD simulations were specified as the velocity inlet boundary and outflow boundary conditions, respectively. Based on the experiments, the indoor heat sources included the thermal manikins and ceiling lamps, which were set as a constant heat flux boundary condition. In practical engineering, exterior wall temperature would vary with the variations in outdoor meteorological parameters. In this study, only the common wall temperature was investigated. In general, the difference between exterior wall temperature and indoor air temperature should be below 8 °C. ASHRAE specifies a comfortable indoor temperature of 18–24 °C in heating conditions. Therefore, the exterior wall temperature was set as 10–16 °C in this study. The right wall and right window are mainly used to study the influence of outdoor meteorological parameters on the temperature distribution. Therefore, the right wall and right window are regarded as the enclosure structure. Furthermore, in each case, the enclosure structure is defined as a constant wall temperature. The effects of outdoor weather conditions on the

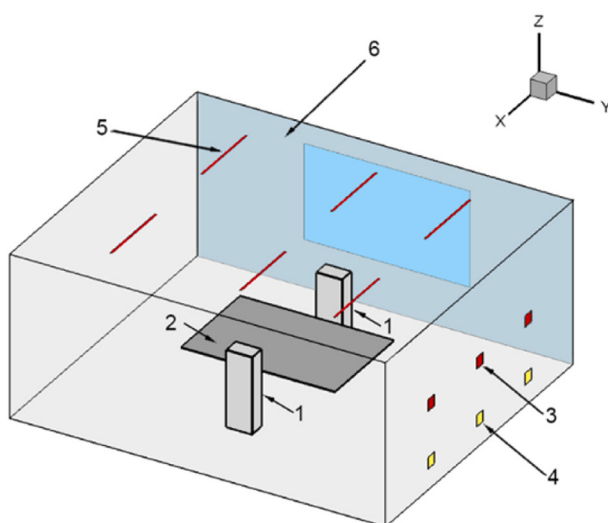


**Fig. 1.** Setup of test chamber. (1: thermal manikin, 2: desk, 3: double-deflection grille diffusers (air inlets), 4: air outlets, 5: lamp, 6: right wall).

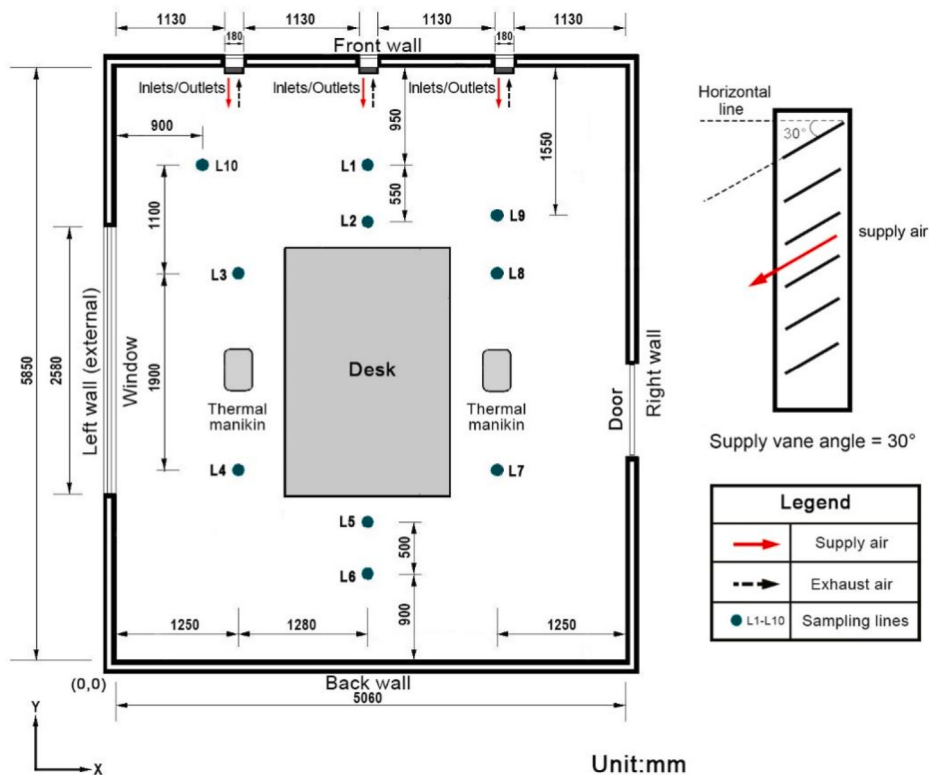


Fig. 2. Diagram of test chamber.

**Table 2**  
Information on three experimental cases.

Number	Supply air velocity/ m/s	Supply air temperature/°C	Right wall temperature/°C	Right window temperature/°C
Case A	1.42	26	20.53	18.57
Case B	0.92	26	20.38	18.67
Case C	1.42	24	19.75	18.75

indoor environment were obtained by varying the wall temperature [38, 39]. The other walls, floor, and ceiling were defined to be adiabatic. The boundary conditions are presented in Table 3.

This study focused on the temperature distribution in the occupied zone (0.1 m from the exterior wall, 0.3 m from the inner wall, and 1.7 m in height) under SV heating. All the simulated measuring points were uniformly arranged in the occupied zone.

### 2.2.2. Solver settings

The airflow in the test chamber was steady, incompressible, and turbulent. Because the test chamber was supposed to maintain a marginally positive pressure, the effect of the cold air infiltration could be negligible. According to previous researches, the standard  $k-\epsilon$  model is slightly better than the RNG  $k-\epsilon$  and Realizable  $k-\epsilon$  models for

predicting the distributions of air velocity and temperature under SV [40]. Thus, the standard  $k-\epsilon$  two-equation turbulence model was used in this study. The standard wall function was employed to simulate the turbulent flow near the wall. Inflation layers were developed around the thermal and fluid boundary layers, and the non-dimensional wall distance,  $y+$ , was below five [38]. The discrete ordinates (DO) model was used to calculate the radiation heat transfer. The buoyancy effect was considered using the Boussinesq model [38]. A second-order upwind scheme was used to discretize the momentum, energy, and turbulence equations. The pressure–velocity coupling method was SIMPLE-C. The energy-scaled residuals were set as  $1 \times 10^{-6}$ , and the other scale residuals were less than  $1 \times 10^{-4}$ . For stable convergence, the under-relaxation factors for the pressure, momentum, turbulent kinetic energy, turbulent dissipation rate, and turbulent viscosity were changed to 0.3, 0.7, 0.8, 0.8, and 0.6, respectively.

### 2.2.3. Grid-independent tests

For the grid-independent tests, a CFD model with 1338804 (coarse), 2696760 (moderate), and 3799892 (fine) hexahedron grids were selected for comparison. The thermal and fluid boundary layers of the heat sources such as the air inlets, thermal manikin, lamp, and exterior wall were refined (see Fig. 3) to capture the details of the flow variables. The air velocities and temperature distribution of the three grids under identical conditions were compared, as shown in Fig. 4. The results show that the airflow velocities and temperatures predicted using the moderate grid were close to those obtained using the fine grid, whereas the air temperature calculated using the coarse grid was significantly different from that obtained using the fine grid. Therefore, the moderate grid was adopted considering both prediction accuracy and calculation cost. The element quality was higher than 0.9.

### 2.2.4. Studied cases

An orthogonal design was used in this study to reduce the number of CFD simulation cases. In general, the supply vane angle should be downward considering the influence of thermal buoyancy [26]. To fully

**Table 3**  
Boundary conditions of computational fluid dynamics (CFD) simulations.

Name of Boundary	Boundary type
Room air inlet	Inlet velocity
Room air outlet	Outflow
Room window	Constant wall temperature
Room right wall	Constant wall temperature
Occupant	Constant heat flux, 60 W/m <sup>2</sup>
Ceiling lights	Constant heat flux, 639 W/m <sup>2</sup>
Other room walls	Adiabatic wall

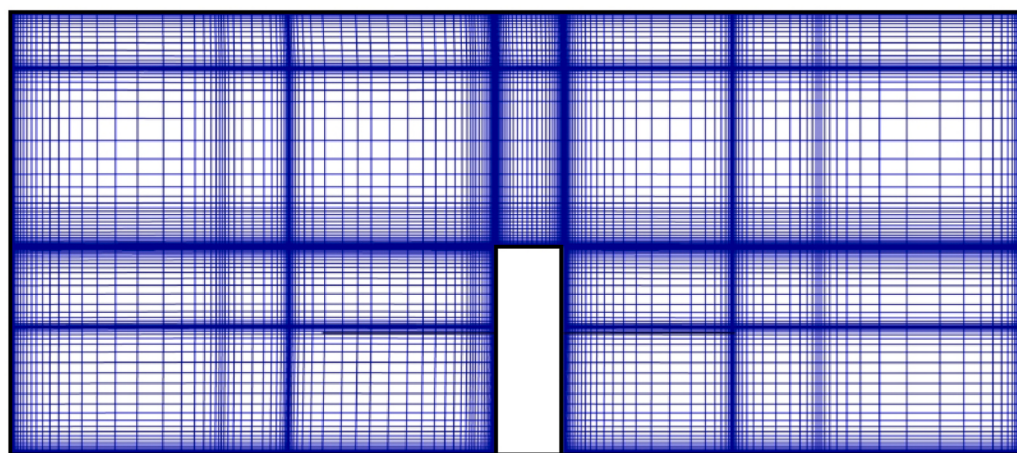


**Fig. 3.** Mesh of computational domain ( $X = 1.2$  m).

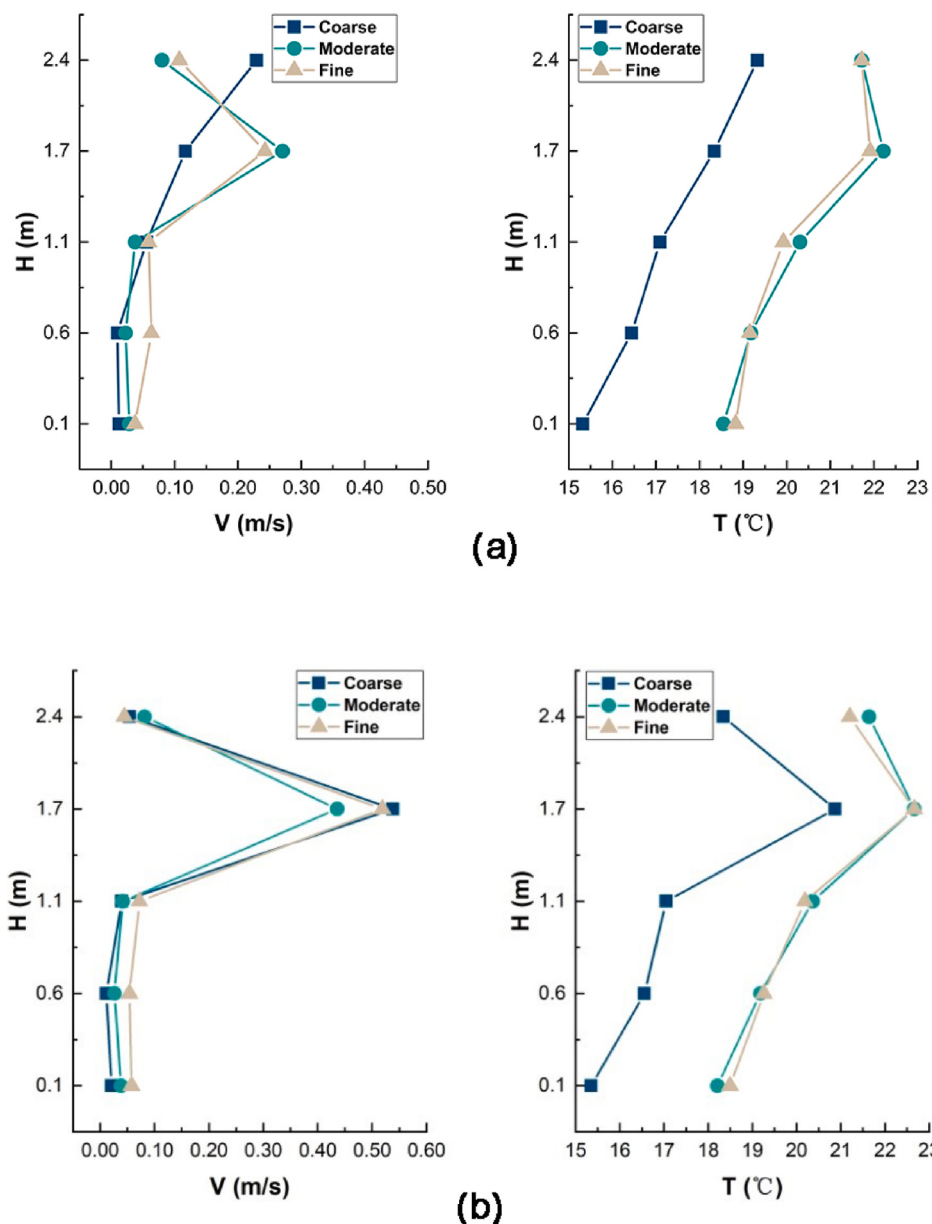


**Fig. 4.** Grid-independent tests. (a) Sampling Line 7; and (b) Sampling Line 9.

consider the influence of the air supply angle on the air temperature uniformity, the supply vane angle was set as 0°–60° in this study. An excessively low air supply temperature can result in draft discomfort [22], whereas an excessively high temperature would cause the supply air to flow directly upward to the upper area [26]. Therefore, the air supply temperature was set as 23–29 °C. In general, the flow upwards of warm air can be largely reduced when the air velocity is higher than 1 m/s [30]. However, the occupants are likely to experience draft discomfort when the supply air velocity is above 2 m/s [24]. Therefore, the supply air velocity in this study was set as 0.9 m/s–1.8 m/s. In this study, the right wall temperature was set as 10–16 °C, as shown in Table 4. The simulation conditions in this study addressed all the common conditions in winter.

### 2.3. Grey relational analysis

Grey relational analysis (GRA) is a method for analyzing the correlations between comparative parameters and reference parameters. It is a significant part of the grey system theory proposed by Deng in 1982 [41]. It uses a small dataset (the number of data elements can be four), and is not required to strictly adhere to certain statistical laws for analyzing the correlation degrees between reference parameters and comparative parameters even in a deficient, incomplete, and uncertain system [42]. Therefore, the correlation degree between the reference parameters and comparative parameters can be non-linear [43]. The degree of correlation is expressed by the grey relational grade (GRG) [44].

The GRA has a wide range of applications such as in agriculture, economics, geography, medicine, meteorology, and earthquakes [41]. In this study, the GRA was used to obtain the degrees of importance of the respective parameters (i.e., supply air velocity, supply air temperature, supply vane angle, and exterior wall temperature) with regard to their effects on the air temperature uniformity in the occupied zone. The procedure for GRA is as follows:

**Step 1.** Determine the reference parameters that reflect the characteristics of the system and the comparative parameters that affect the system.

**Step 2.** Normalize the data to remove the dimensions of each parameter, i.e., to obtain a correct conclusion while comparing. Use the average value method of normalization:

$$x'_0(k) = \frac{x_0(k)}{\sum_{k=1}^n x_0(k)} \quad (1)$$

**Table 4**  
Orthogonal design conditions.

Case	Supply vane angle/°	Supply air temperature/°C	Supply air velocity/m/s	Exterior wall temperature/°C
1	0	23	0.9	10
2	0	25	1.2	12
3	0	27	1.5	14
4	0	29	1.8	16
5	20	23	1.2	14
6	20	25	0.9	16
7	20	27	1.8	10
8	20	29	1.5	12
9	40	23	1.5	16
10	40	25	1.8	14
11	40	27	0.9	12
12	40	29	1.2	10
13	60	23	1.8	12
14	60	25	1.5	10
15	60	27	1.2	16
16	60	29	0.9	14

$$x'_i(k) = \frac{x_i(k)}{\sum_{k=1}^n x_i(k)} \quad (2)$$

In the above,  $x_0(k)$  and  $x_i(k)$  are the original reference parameters and comparative parameters, respectively.  $x'_0(k)$  and  $x'_i(k)$  are the normalized reference parameters and comparative parameters, respectively.

**Step 3.** Calculate the grey relational coefficient  $\varepsilon_{0i}(k)$  between  $x'_0(k)$  and  $x'_i(k)$  at Point  $k$ . It expresses the distance between the two factors:

$$\varepsilon_{0i}(k) = \frac{\min_i \min_k |x'_0(k) - x'_i(k)| + \rho \max_i \max_k |x'_0(k) - x'_i(k)|}{|x'_0(k) - x'_i(k)| + \rho \max_i \max_k |x'_0(k) - x'_i(k)|} \quad (3)$$

In the above,  $|x'_0(k) - x'_i(k)|$  is the absolute value of the difference between  $x'_0(k)$  and  $x'_i(k)$  at Point  $k$ ,  $\min_i \min_k |x'_0(k) - x'_i(k)|$  is the minimal value of  $|x'_0(k) - x'_i(k)|$ , and  $\max_i \max_k |x'_0(k) - x'_i(k)|$  is the maximal value of  $|x'_0(k) - x'_i(k)|$ .  $\rho$  is a distinguishing coefficient used to adjust the differences in the significance of the results [45]. It is generally set to 0.5.

**Step 4.** Calculate the GRG. It is necessary for transforming each grey relational coefficient at each point into an average value.  $\gamma_{0i}$  represents the GRG:

$$\gamma_{0i} = \frac{1}{n} \sum_{k=1}^n \varepsilon_{0i}(k) \quad (4)$$

here,  $n$  is the number of simulation groups.

The GRGs reflect the importance of the comparative parameters on the reference values.  $\gamma_{0i}$  is between zero and one. The higher the GRG, the closer is the relationship between the parameter and reference value. Therefore, the GRG is a good index for determining which parameters are more important to the air temperature uniformity in the occupied zone under SV heating.

## 3. Results and discussion

### 3.1. Experimental results

#### 3.1.1. Horizontal distribution of air temperature

In this study, the SD and extremum air temperature difference are used to evaluate the fluctuations in the local air temperature at each height. Fig. 5 shows the local air temperature of each measuring point at the heights of 0.1 m, 0.6 m, 1.1 m, and 1.7 m in the three experimental cases. On the 0.1 m-high plane, the extremum air temperature differences ( $T_{\max-\min}$ ) of the measuring points corresponding to Cases A, B, and C are 1.9 °C, 1.1 °C, and 1.2 °C, respectively. On the 0.6 m-high plane, the values are slightly higher, i.e., 1.8 °C, 1.4 °C, and 1.8 °C, respectively. On the 1.1 m-high plane, the values are 0.4 °C, 1.1 °C, and 0.9 °C, respectively. On the 1.7 m-high plane,  $T_{\max-\min}$  fluctuates in the range 0.5–0.7 °C. The calculated results for the SDs of the air temperatures at each height are shown in Fig. 5. For Cases A, B, and C, the horizontal air temperature SD ( $SD_h$ ) on the 0.1 m-, 0.6 m-, 1.1 m-, and 1.7 m-high planes are in the ranges 0.4–0.6 °C, 0.5–0.6 °C, 0.1–0.4 °C, and 0.1–0.2 °C, respectively.

The results show that the local air temperature on the 0.6 m-high plane displays the maximum fluctuation. This is followed by the 0.1 m-high plane. This is mainly because the air supply diffusers are set at a height of 1.3 m on the front wall, and the supply vane angle in the experimental case is 30° downward horizontally. This causes the warm airflow to be directly sent to the area below 1.1 m of the occupied zone. Thus, the air temperature on the plane below 1.1 m fluctuates significantly. In addition, the two thermal manikins influence the surrounding air temperature distribution, thereby causing the air temperature fluctuations in the lower area to be more evident. It can also be observed

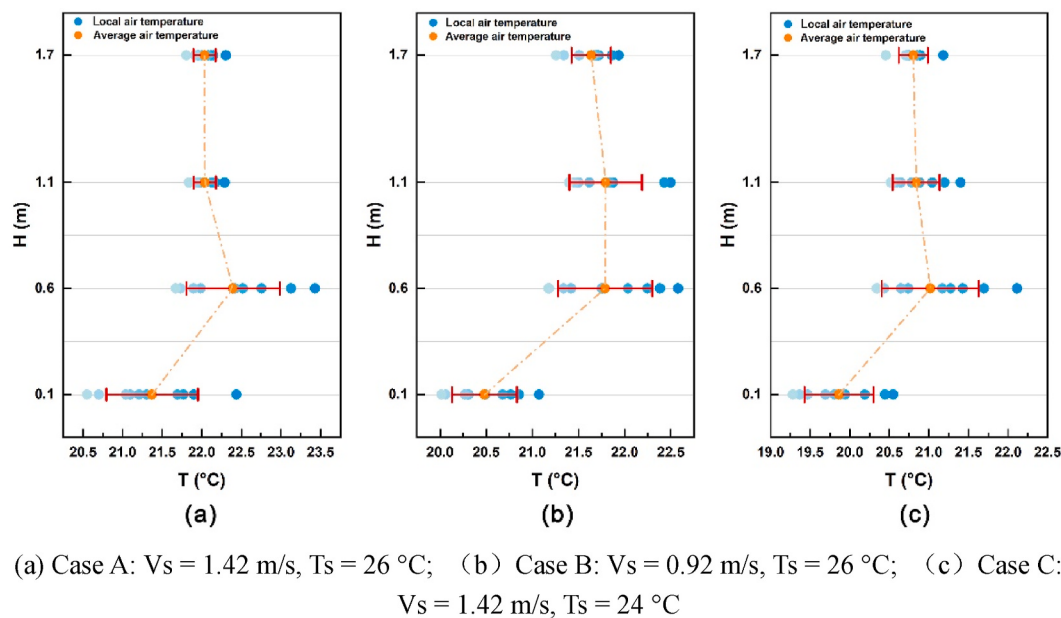


**Fig. 5.** Local air temperature at heights of 0.1 m, 0.6 m, 1.1 m, and 1.7 m in the three experimental cases.

that the SDs of the measured air temperatures on the 0.6 m-, 1.1 m-, and 1.7 m-high planes decrease successively. The main reason for this is that the air distribution in the upper space is less affected by the supply air flow. Furthermore, the effect of thermal buoyancy is significant. The warm air easily converges in the upper space, which results in a more uniform air temperature distribution with an increase in height above 0.6 m.

### 3.1.2. Vertical distribution of air temperature

The vertical air temperature difference can be used to characterize the fluctuation of the air temperature distribution in the vertical direction. Therefore, the vertical air temperature differences between 0.6 m and 0.1 m, 1.1 m and 0.1 m, 1.7 m and 0.1 m on each measuring line are used as reference indexes for analyzing the vertical air temperature distributions in the room equipped with the SV heating system. The calculated results are shown in Fig. 6. For Cases A, B, and C, the average values of the vertical air temperature differences between 0.6 m and 0.1 m are relatively higher, i.e., 1 °C, 1.3 °C, and 1.2 °C, respectively. In contrast, the average vertical air temperature differences between 1.7 m

and 0.1 m are relatively lower: 0.7 °C, 1.1 °C, and 0.9 °C, respectively. The average vertical air temperature differences between 1.1 m and 0.1 m are 0.7 °C, 1.3 °C, and 1 °C, respectively. For all the cases, the vertical temperature stratifications at occupants' positions are less than 3 °C. This is lower than the acceptable threshold of occupants recommended by ASHRAE-55.

The three points worthy of attention are identified by comparing the three cases as follows. First, it can be observed from Figs. 5 and 6 that the variation in air temperature from 0.6 m-high plane to 1.7 m-high plane is not evident. Second, the air temperature distribution in Case A is more uniform than that in Case B. This indicates that the air temperature distribution in the SV heated room can be affected by the supply air parameters. Third, the difference in air temperature uniformity between Cases A and C is smaller than that between Cases A and B. This indicates that an alteration of certain air supply parameters can reduce temperature fluctuations more effectively than that of others.

To summarize, the supply air parameters can affect the uniformity of the temperature distribution. Furthermore, different supply air parameters have different correlation grades with the uniformity of the temperature distribution. Owing to the limited number of experimental cases, it is not feasible to comprehensively analyze the characteristics of the air temperature distribution in the occupied zone under the SV heating mode. The analysis is discussed further in the following sections.

### 3.2. CFD simulations results

#### 3.2.1. Model validation

To validate the CFD simulations, the predicted air temperatures and velocities are compared with the measured values, as shown in Figs. 7 and 8. For air temperature, the predicted results of the CFD are consistent with the measured values. The average difference between the predicted and experimental results is 0.35 °C. For air velocity, the average difference between the predicted and experimental results for all the measuring points is 0.06 m/s, and the maximum difference is 0.21 m/s. Overall, the predicted results are consistent with the experimental results. However, some discrepancies in air temperature and velocity occur at the measuring points below the height of 0.6 m for Sampling Lines 3 and 8. This may be because Sampling Lines 3 and 8 were close to the table and occupants. Thus, a boundary layer separation occurred, where the airflow was complex and unstable. Moreover, the CFD simulation was simplified by omitting the effect of infiltration,

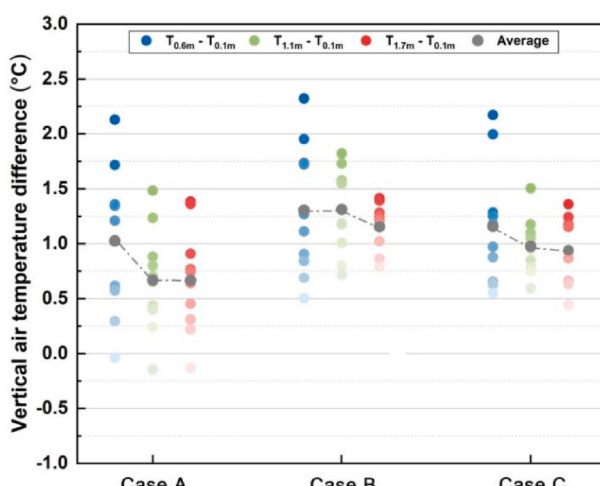


**Fig. 6.** Vertical air temperature differences between 0.6 m and 0.1 m, 1.1 m and 0.1 m, and 1.7 m and 0.1 m.

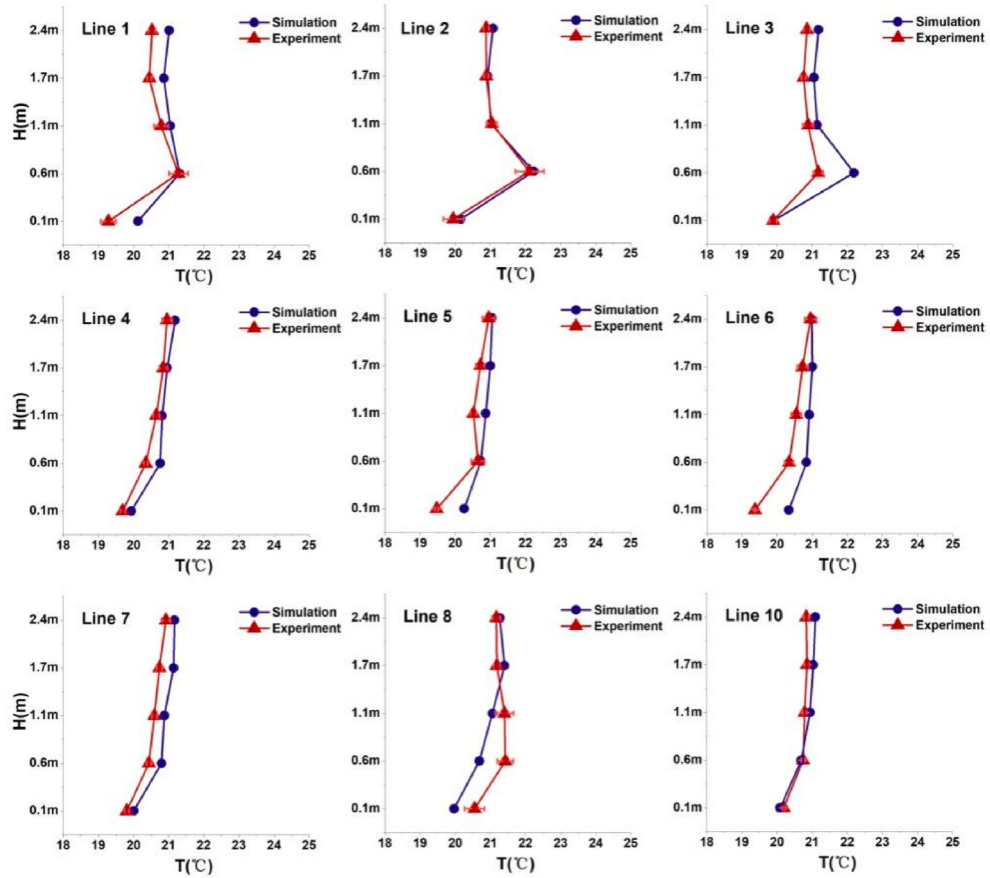


**Fig. 7.** Comparison between results of computational fluid dynamics (CFD) simulations and experiments on local air temperature.

which may also cause the difference between the predicted and measured results.

The results calculated by CFD simulations are in good agreements with the measured data. This reveals that the CFD model established in this study can be reliably used to simulate the indoor air distribution under SV heating mode.

### 3.2.2. Horizontal and vertical distributions of air temperature

To more comprehensively study the horizontal and vertical distributions of temperature in the occupied zone under SV heating in winter, the points were separated by a uniform distance in the occupied zone while analyzing the CFD simulation results. For the horizontal distribution of air temperature, the SD values and extremum air temperature differences at the four heights are listed in Table 5. The smaller the SD values and extremum air temperature differences are, the more uniform the air temperature distribution in the horizontal direction is.

As shown in Table 5, the air temperature SD ranges at the heights of 0.1 m, 0.6 m, 1.1 m, and 1.7 m for the different cases are 0.2–1.19 °C, 0.14–1.49 °C, 0.15–0.87 °C, and 0.08–0.43 °C, respectively. The horizontal extremum air temperature differences at the heights of 0.1, 0.6, 1.1, and 1.7 m are 0.92–3.69 °C, 0.62–6.26 °C, 0.6–3.37 °C, and 0.34–1.86 °C, respectively. For the different cases, the minimum SD and extremum temperature differences at each height are 0.08 °C and 0.34 °C, respectively. That is, in certain cases, the horizontal indoor air temperature distribution is fairly uniform. However, the maximum values of the SD and extremum temperature differences can attain 1.49 °C and 6.26 °C, and the temperature gradient can attain 9.94 °C/m. It is evident that the horizontal distribution of the air temperature is non-uniform in certain cases. This indicates that SV can produce evidently different air temperature distributions for different conditions.

The results show that under different air supply parameters and

outdoor conditions, the 0.6 m-high plane shows the maximum non-uniformity, and the 1.7 m-high plane shows the maximum uniformity. The 0.6 m-high plane in Case 12 exhibits the maximum non-uniformity, as shown in Fig. 9. The plane with the best uniformity is at the height of 1.7 m in Case 16, as shown in Fig. 10. This may be because the supply vane was turned downward to suppress the influence of thermal buoyancy and the momentum of air supply decreases with an increase in the air supply distance. In addition, the heat dissipation of the human body may also affect the air temperature distribution. The air temperature at 0.6 m fluctuates significantly owing to the multiple influences of thermal buoyancy, air supply momentum, and human body heat dissipation. However, by adjusting the air supply parameters, the SD value of the horizontal air temperature at 0.6 m can be reduced to 0.14 °C (such as in Case 1) to achieve better uniformity. In addition, most of the cases show that the uniformity of the horizontal air temperature increases with an increase in height above 1.1 m. The main reasons are that the upper space is less affected by the airflow and human body heat dissipation, and the hot air converges in the upper part owing to the influence of thermal buoyancy. Thus, the air temperature fluctuation is moderate. Therefore, the results obtained using different parameter settings show that the air supply parameters and outdoor conditions have significant relationships with the uniformity of horizontal air temperature under stratum ventilation. However, the specific influence of each parameter on the air temperature distribution can be determined using GRA as discussed below.

For the air temperature distribution in the vertical direction, the average air temperatures at the four heights (i.e., 0.1 m, 0.6 m, 1.1 m, and 1.7 m) in each case and vertical air temperature differences between 0.6 m and 0.1 m, 1.1 m and 0.1 m, and 1.7 m and 0.1 m are shown in Table 6. For Case 13, the air temperature differences between the different heights and the height of 0.1 m are the smallest: the average air

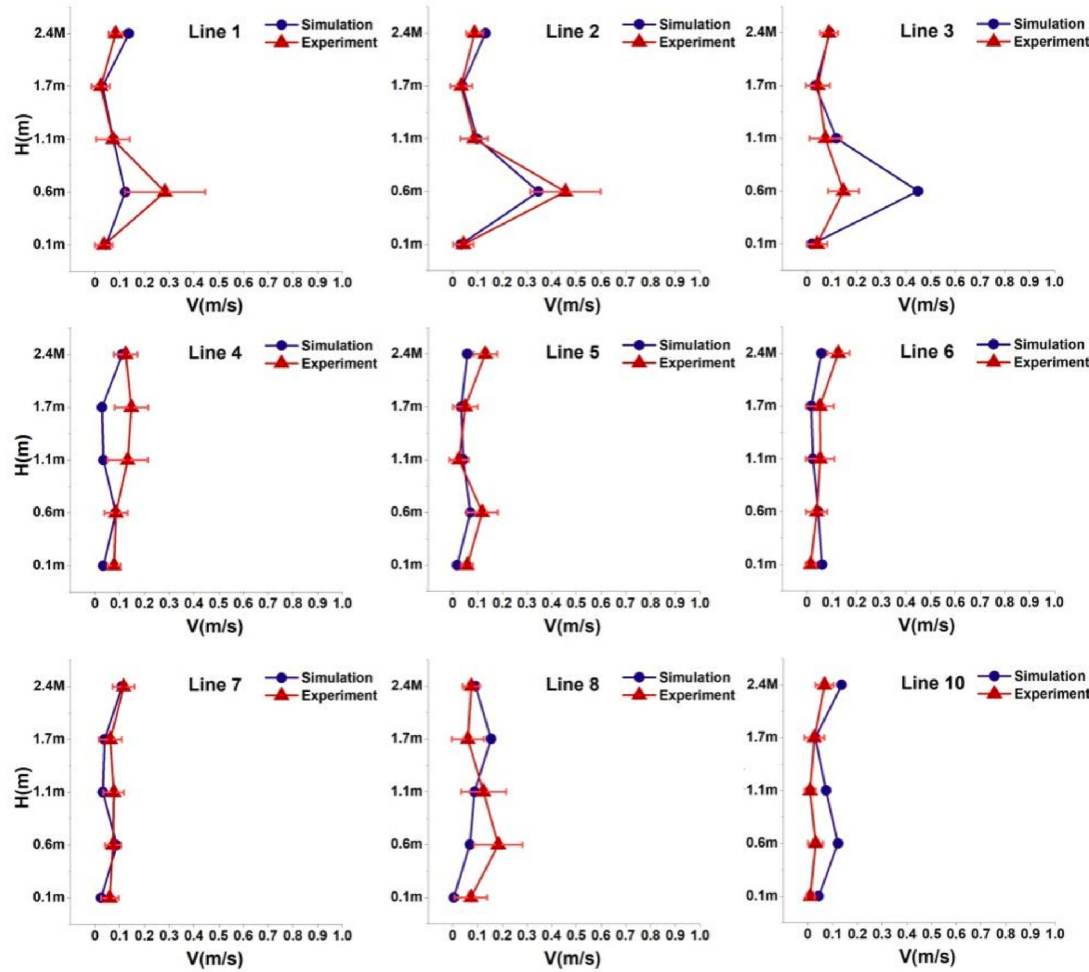


Fig. 8. Comparison between results of CFD simulations and experiments on local air velocity.

**Table 5**

Simulation results for horizontal distribution of air temperature (SD: standard deviation).

Case	SD <sub>0.1</sub> /°C	SD <sub>0.6</sub> /°C	SD <sub>1.1</sub> /°C	SD <sub>1.7</sub> /°C	(T <sub>max-min</sub> ) <sub>0.1</sub> /°C	(T <sub>max-min</sub> ) <sub>0.6</sub> /°C	(T <sub>max-min</sub> ) <sub>1.1</sub> /°C	(T <sub>max-min</sub> ) <sub>1.7</sub> /°C
1	0.27	0.14	0.20	0.43	1.09	0.62	0.60	1.77
2	0.31	0.27	0.33	0.43	1.42	0.94	1.18	1.86
3	0.51	0.39	0.30	0.32	1.83	1.24	0.96	1.28
4	0.63	0.39	0.28	0.25	2.25	1.43	0.92	1.04
5	0.26	0.26	0.34	0.13	0.93	1.14	1.61	0.57
6	0.25	0.24	0.71	0.19	1.11	0.74	2.41	0.72
7	0.64	0.63	0.52	0.21	3.00	2.64	2.42	0.82
8	0.49	0.36	0.87	0.27	2.14	1.72	3.37	0.93
9	0.74	0.41	0.28	0.16	2.01	1.43	1.22	0.65
10	1.19	0.63	0.45	0.24	3.69	2.55	2.40	1.00
11	0.23	0.22	0.51	0.32	1.10	0.94	2.34	1.40
12	0.28	1.49	0.66	0.28	1.19	6.26	2.61	1.32
13	0.64	0.31	0.25	0.29	2.55	1.42	1.03	0.96
14	0.36	0.30	0.23	0.16	1.54	1.37	1.07	0.62
15	0.20	0.28	0.19	0.13	0.94	1.24	0.81	0.51
16	0.20	0.15	0.15	0.08	0.92	0.63	0.91	0.34

temperature difference is only 0.07 °C. This showed a good vertical uniformity, as shown in Fig. 11. For Case 1, the air temperature differences between the different heights and the height of 0.1 m are the largest: the average air temperature difference is 2.30 °C. This results in an evident vertical stratification, as shown in Fig. 12. A comparison of Cases 13 and 1 clearly reveals the difference in the vertical air temperature distribution, as shown in Figs. 11 and 12. Therefore, different parameter settings result in different vertical air temperature

distributions.

The average vertical air temperature differences between 0.6 m and 0.1 m, 1.1 m and 0.1 m, and 1.7 m and 0.1 m are in the range 0.11–1.79 °C, 0.04–2.31 °C, and 0.06–3.51 °C, respectively. The average vertical air temperature difference between 1.7 m and 0.1 m is the largest, which is consistent with the previous study [23]. This may be because when the air supply parameter settings are unsuitable, thermal buoyancy would cause the direct elevation of the warm air, ineffective

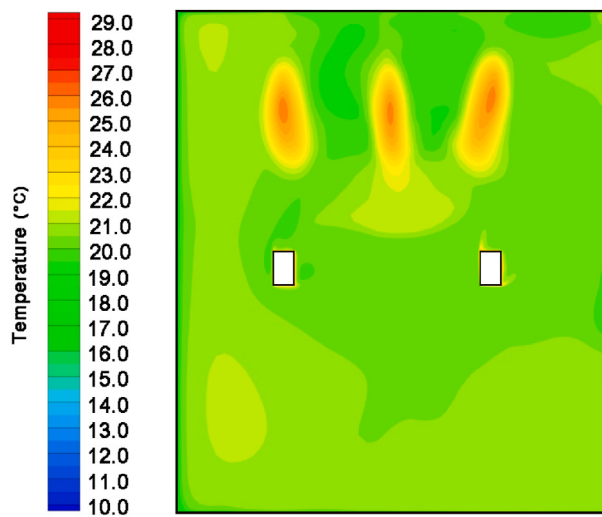


**Fig. 9.** Horizontal distribution of air temperature in Case 12 ( $Z = 0.6$  m).

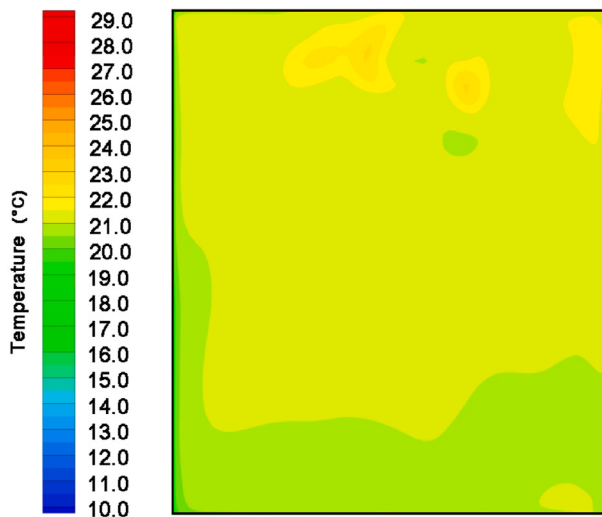


**Fig. 10.** Horizontal distribution of air temperature in Case 16 ( $Z = 1.7$  m).

heating of the lower zone, and concentration of the warm air in the upper part of the room. Accordingly, the vertical air temperature difference between 1.7 m and 0.1 m is larger, and the maximum vertical temperature gradient can attain  $2.19^{\circ}\text{C}/\text{m}$ . A vertical temperature

difference of over  $3^{\circ}\text{C}$  may cause thermal discomfort. Thus, the parameter settings can significantly affect the vertical air temperature distribution, and thereby affect the thermal comfort of occupants.

**Table 7** shows that the average maximum air temperature gradient in the horizontal direction  $\Delta T_h$  is  $3.46^{\circ}\text{C}/\text{m}$ ; and the average maximum air temperature gradient in the vertical direction  $\Delta T_v$  is  $2.44^{\circ}\text{C}/\text{m}$ . Under the different heating conditions in winter, the temperature uniformity in the horizontal direction is worse than that in the vertical direction. That is, under SV heating in winter, it is easier to achieve air temperature uniformity in the vertical direction than in the horizontal direction. This is similar to the cooling conditions for SV in summer [46]. Therefore, for winter heating conditions, attentions should be paid to the effects of the air supply parameters on the temperature uniformity. If the air supply parameters (i.e., supply vane angle, supply air temperature, and supply air velocity) are not coupled effectively, the horizontal and vertical air temperature distributions may be non-uniform, especially for the horizontal air temperature distributions.

### 3.2.3. Energy savings

The energy utilization coefficient (EUC) is generally used to quantify the efficiency of energy utilization in a ventilation system [26]. In general, when  $\text{EUC} > 1$ , the larger the EUC is, the air distribution is more energy efficient.

$$\text{EUC} = \frac{t_s - t_e}{t_s - t_a} \quad (5)$$

where  $t_s$  is the supply air temperature,  $^{\circ}\text{C}$ ;  $t_a$  is the average air temperature in the occupied zone,  $^{\circ}\text{C}$ ; and  $t_e$  is the exhaust air temperature,  $^{\circ}\text{C}$ .

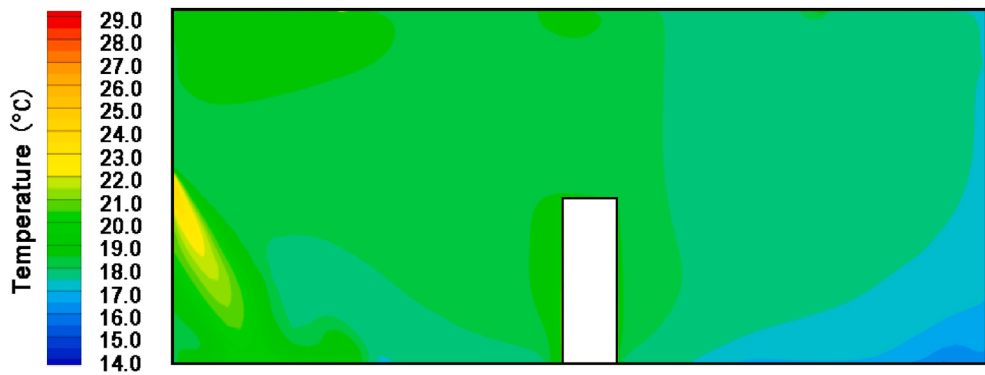
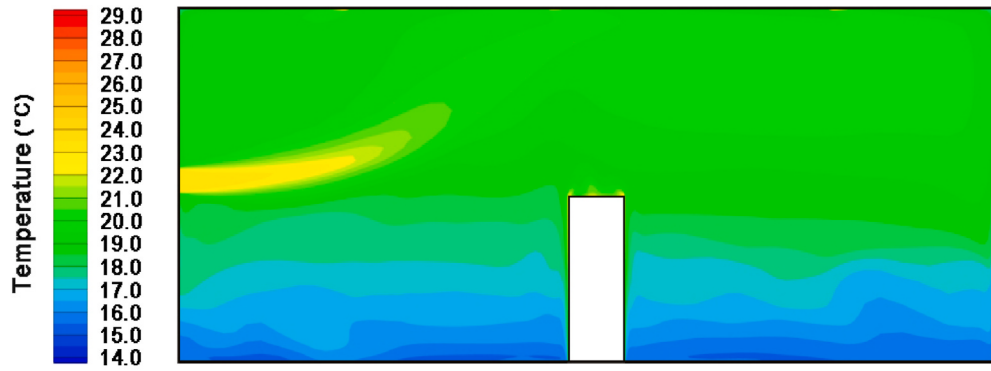
**Fig. 13** shows the EUC for each case. In 13 of the 16 cases, EUC was higher than one, and attained a maximum value of 1.23. In other words, energy savings could be achieved in 81.25% of these cases. It indicates that energy can be saved by using SV for heating when the air supply parameter settings are reasonable. However, EUC was less than one for Cases 13–15, wherein the supply air vane angle applied was  $60^{\circ}$ , and in this study, SV adopted the same-side return air as the supply airflow. This large vane angle of the air supply may result in short circuiting between supply airflow and exhaust airflow, and thereby increasing the energy consumption. Although the supply air vane angle of Case 16 was  $60^{\circ}$ , it could attain an EUC of 1.07 owing to its effective coupling with the supply air velocity and supply air temperature. Therefore, it is necessary to pay attentions on the coupling of air supply parameters whilst using SV heating to improve air temperature uniformity, realize the thermal comfort requirements, and achieve energy savings.

### 3.3. Grey relational analysis

Equations (1)–(4) of the GRA and CFD simulation results are used to

**Table 6**  
Simulation results for vertical distribution of air temperature.

Case	$T_{0.1\text{m\_ave}}/^{\circ}\text{C}$	$T_{0.6\text{m\_ave}}/^{\circ}\text{C}$	$T_{1.1\text{m\_ave}}/^{\circ}\text{C}$	$T_{1.7\text{m\_ave}}/^{\circ}\text{C}$	$T_{0.6\text{m\_ave}} - T_{0.1\text{m\_ave}}/^{\circ}\text{C}$	$T_{1.1\text{m\_ave}} - T_{0.1\text{m\_ave}}/^{\circ}\text{C}$	$T_{1.7\text{m\_ave}} - T_{0.1\text{m\_ave}}/^{\circ}\text{C}$	$\Delta T_{\text{ave}}/^{\circ}\text{C}$
1	15.96	17.06	18.24	19.46	1.10	2.28	3.51	2.30
2	19.23	20.02	20.74	21.47	0.79	1.51	2.24	1.51
3	21.76	22.75	23.09	23.62	0.99	1.33	1.86	1.39
4	24.37	25.20	25.47	25.86	0.83	1.10	1.49	1.14
5	19.37	20.07	20.57	20.50	0.70	1.20	1.13	1.01
6	20.89	21.42	22.20	22.20	0.53	1.31	1.31	1.05
7	20.58	21.85	22.42	22.26	1.27	1.84	1.68	1.60
8	21.61	22.67	23.92	23.72	1.06	2.31	2.11	1.82
9	20.92	21.05	21.15	21.09	0.13	0.23	0.16	0.18
10	21.66	21.79	21.87	21.82	0.14	0.21	0.17	0.17
11	18.47	19.29	20.33	20.73	0.82	1.86	2.26	1.65
12	18.94	20.73	21.14	21.38	1.79	2.20	2.45	2.14
13	17.96	18.07	17.99	18.01	0.11	0.04	0.06	0.07
14	16.37	17.01	17.36	17.81	0.64	0.99	1.44	1.02
15	20.82	21.38	21.67	21.72	0.56	0.85	0.90	0.77
16	19.56	20.24	20.72	20.95	0.68	1.15	1.38	1.07

Fig. 11. Vertical distribution of air temperature in Case 13 ( $X = 1.25\text{ m}$ ).Fig. 12. Vertical distribution of air temperature in Case 1 ( $X = 1.25\text{ m}$ ).

**Table 7**  
Comparison of vertical and horizontal air temperature distributions.

Case	$\Delta T_h/\text{°C/m}$	$\Delta T_v/\text{°C/m}$
1	0.36	2.22
2	0.82	1.50
3	0.84	1.49
4	0.49	1.23
5	0.50	1.10
6	1.19	1.06
7	0.92	1.81
8	1.91	1.92
9	0.59	0.20
10	1.15	0.20
11	0.75	1.64
12	3.46	2.44
13	0.46	0.10
14	0.39	1.06
15	0.35	0.84
16	0.27	1.12

Note:  $\Delta T_h$  — average maximum temperature gradient in each plane in the horizontal direction,  $^{\circ}\text{C}/\text{m}$ ;  $\Delta T_v$  — average maximum temperature gradient in the vertical direction,  $^{\circ}\text{C}/\text{m}$ .

calculate the GRGs between the influencing parameters (i.e., supply vane angle, supply air temperature, supply air velocity, and wall surface temperature) and  $T_{(\max-\min)0.1}$ ,  $T_{(\max-\min)0.6}$ ,  $T_{(\max-\min)1.1}$ , and  $T_{(\max-\min)1.7}$ . The results can be used to characterize the correlations between the horizontal air temperature uniformity and influencing parameters. The calculation results are shown in Fig. 14.

For horizontal air temperature uniformity on the 0.1 m-, 0.6 m-, and 1.1 m-high planes, the relational grade of the supply air velocity is the highest (GRG values of 0.82, 0.83, and 0.65, respectively), whereas that of the supply vane angle is the lowest (GRG values of 0.53, 0.68, and 0.54, respectively). The relational grades of the supply air

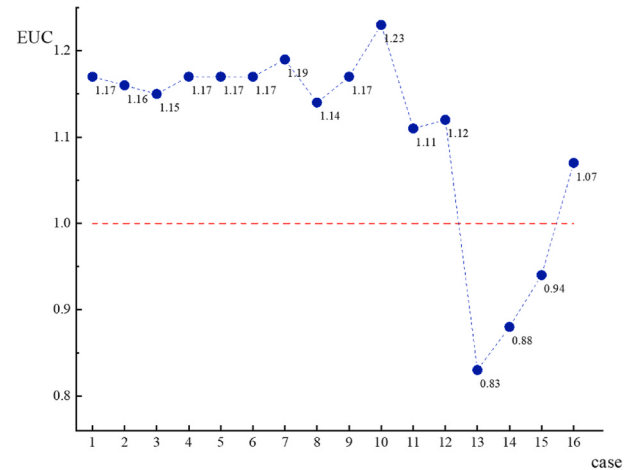
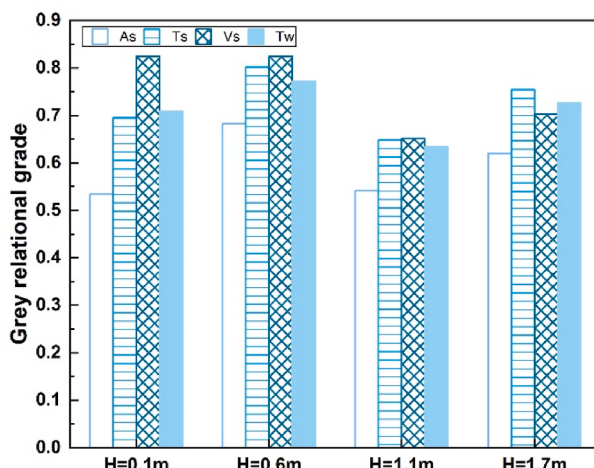


Fig. 13. EUC in sixteen simulation cases.

and exterior wall temperature are highly similar. However, the results obtained from the 1.7 m-high plane differ from those for the planes at the other three heights. The supply air temperature has the largest influence on the uniformity of the horizontal air temperature on the 1.7 m-high plane (GRG = 0.75). It is followed by the exterior wall temperature (GRG = 0.73), supply air velocity (GRG = 0.70), and then supply vane angle (GRG = 0.62).

The GRG between supply air velocity and horizontal air temperature uniformity (GRG = 0.82) is significantly higher than that between the supply air temperature and horizontal air temperature uniformity (GRG = 0.70) on the 0.1 m-high plane. However, this difference decreases gradually as the height increases. The GRG between the supply air



**Fig. 14.** Grey relational grades of supply air parameters and exterior wall temperature on horizontal air temperature uniformity.

temperature and air temperature uniformity ( $\text{GRG} = 0.75$ ) is higher on the 1.7 m-high plane. This is because the warm air flows downward into the occupied zone from the 1.3 m height on the front wall. The lower zone is mainly affected by the initial momentum of the airflow. Thus, the supply air velocity is the main factor that affects the horizontal air temperature uniformity, rather than the thermal buoyancy caused by the air temperature. With an increase in height, the thermal buoyancy gradually becomes the dominant factor. Meanwhile, the influence of the initial momentum gradually weakens, which causes the influence of the supply air velocity on the upper zone to decrease gradually and that of the supply air temperature to increase gradually [47]. This explains the unique results of the GRA of the horizontal air temperature uniformity at the height of 1.7 m.

The average air temperature differences between the planes at the heights of 0.6 m and 0.1 m, 1.1 m and 0.1 m, and 1.7 m and 0.1 m are calculated. The GRGs between these results and the four parameters (i.e., supply vane angle, supply air temperature, supply air velocity, and exterior wall temperature) are also calculated. The results could be used to characterize the correlations of these four parameters with the vertical air temperature uniformity, as shown in Fig. 15. The GRG of the supply air temperature is the highest (GRG values of 0.76, 0.73, and 0.74, respectively), that of the supply vane angle is the lowest (GRG values of 0.59, 0.54, and 0.52, respectively), and those of the exterior wall temperature and supply air velocity are approximately equal (GRGs close to 0.7). This indicates that a reduction in the supply air temperature can more effectively reduce the differences in vertical air temperature. This conclusion is consistent with the results of the existing researches [24,26,27].

#### 4. Conclusions

In this study, the uniformity of the air temperature distributions in the occupied zone of an SV heated room was studied based on the experimental and numerical simulation methods. The relational grades for three air supply parameters (supply air temperature, supply air velocity, and supply vane angle) and the outdoor environment (exterior wall temperature) with regard to the vertical and horizontal air temperature uniformities were obtained based on a GRA. The main conclusions are as follows:

1. The maximum non-uniformity occurs at the height of 0.6 m in the occupied zone, the SD attains  $1.49^{\circ}\text{C}$ , and the extremum air temperature difference is  $6.26^{\circ}\text{C}$ . The best uniformity is observed at 1.7 m, with an SD of  $0.14^{\circ}\text{C}$  and extremum temperature difference of  $0.62^{\circ}\text{C}$ .

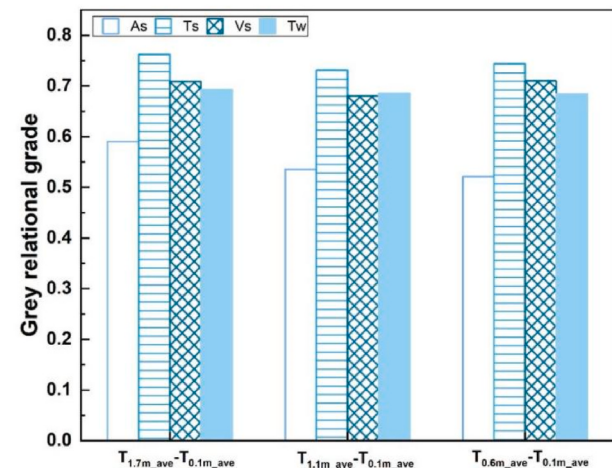


**Fig. 15.** Grey relational grades of supply air parameters and exterior wall temperature on vertical air temperature uniformity.

2. The average maximum air temperature gradient in each plane in the horizontal direction  $\Delta T_h$  is  $3.46^{\circ}\text{C}/\text{m}$ . The average maximum air temperature gradient in the vertical direction  $\Delta T_v$  is  $2.44^{\circ}\text{C}/\text{m}$ . The temperature uniformity in the horizontal direction is inferior to that in the vertical direction.
3. Among the sixteen simulation cases, the EUC of thirteen cases is higher than one and the maximum value is 1.23. This shows that SV can achieve energy savings under heating mode. However, when the coupling of supply air parameters is ineffective, the EUC can be less than one. Therefore, it is crucial to pay attentions to the reasonable selection of ventilation parameters for achieving a more uniform temperature distribution, more comfortable indoor environment, and more energy-efficient system operation.
4. With regard to the uniformity of the vertical and horizontal air temperature distributions in the SV heated room, the influences of the supply air velocity and supply air temperature are relatively larger. These are followed by the exterior wall temperature and then the supply vane angle.

#### Author contribution statement

Junmeng Lyu: Investigation, Data curation, Writing - original draft, Visualization. Xuan Feng: Experiment, Data analysis, Writing - original draft. Yong Cheng: Methodology, Data analysis, Supervision. Chunhui Liao: Conceptualization, Data analysis, Writing - review & editing, Supervision.

#### Declaration of competing interest

The authors declare that they have no known competing financial interests or personal relationships that could have appeared to influence the work reported in this paper.

#### Acknowledgements

The work presented in this paper was financially supported by Scientific Research Foundation for Talented Scholars, Chongqing University of Science and Technology (Grant No. 0206/182003009) and Municipal Innovative Scientific Training Project for college students in Chongqing, China (Grant No. S201910611410).

## References

- [1] H. Liu, Y.X. Wu, B.Z. Li, et al., Seasonal variation of thermal sensations in residential buildings in the Hot Summer and Cold Winter zone of China, *Energy Build.* 140 (2017) 9–18.
- [2] R. Yao, V. Costanzo, X. Li, et al., The effect of passive measures on thermal comfort and energy conservation. A case study of the hot summer and cold winter climate in the Yangtze River region, *J. Build. Eng.* 15 (2018) 298–310.
- [3] M. Laetitia, S. Jiyun, S.C. Alan, et al., The Hot Summer-Cold Winter region in China: challenges in the low carbon adaptation of residential slab buildings to enhance comfort, *Energy Build.* 223 (2020) 110181.
- [4] J. Skoog, N. Fransson, L. Jagemar, Thermal environment in Swedish hospitals: summer and winter measurements, *Energy Build.* 37 (8) (2005) 872–877.
- [5] B. Li, C. Du, R. Yao, et al., Indoor thermal environments in Chinese residential buildings responding to the diversity of climates, *Appl. Therm. Eng.* 129 (2018) 693–708.
- [6] W. Jialin, H. Zhijian, S. Jingyun, et al., A method for the determination of optimal indoor environmental parameters range considering work performance, *J. Build. Eng.* 35 (2021) 101976.
- [7] L. Lan, Z. Lian, L. Pan, et al., Neurobehavioral approach for evaluation of office workers' productivity: the effects of room temperature, *Build. Environ.* 44 (8) (2008) 1578–1588.
- [8] J. Cai, B.Z. Li, W. Yu, et al., Associations of household dampness with asthma, allergies, and airway diseases among preschoolers in two cross-sectional studies in Chongqing, China: repeated surveys in 2010 and 2019, *Environ. Int.* 140 (2020) 105752.
- [9] N. Fransson, D. Västfjäll, J. Skoog, In search of the comfortable indoor environment: a comparison of the utility of objective and subjective indicators of indoor comfort, *Build. Environ.* 42 (5) (2007) 1886–1890.
- [10] D. Tan, B. Li, Y. Cheng, et al., Airflow pattern and performance of wall confluent jets ventilation for heating in a typical office space, *Indoor Built Environ.* 29 (1) (2020) 67–83.
- [11] Y. Fan, X. Li, M. Zheng, et al., Numerical study on effects of air return height on performance of an underfloor air distribution system for heating and cooling, *Energy* 13 (5) (2020) 1070.
- [12] A. Kuesters, A. Woods, A comparison of winter heating demand using a distributed and a point source of heating with mixing ventilation, *Energy Build.* 55 (2012) 332–340.
- [13] E. Arens, H. Zhang, C. Huijenga, Partial- and whole-body thermal sensation and comfort—Part I: uniform environmental conditions, *J. Therm. Biol.* 31 (1) (2006) 53–59.
- [14] K.T. Andersen, Theory for natural ventilation by thermal buoyancy in one zone with uniform temperature, *Build. Environ.* 38 (11) (2003) 1281–1289.
- [15] M. Krajčík, A. Simone, B.W. Olesen, Air distribution and ventilation effectiveness in an occupied room heated by warm air, *Energy Build.* 55 (2012) 94–101.
- [16] ASHRAE: Atlanta GA-USA. UFAD Guide Design, Construction and Operation of Underfloor Air Distribution Systems. 2013.
- [17] T.S. Lim, L. Schaefer, J.T. Kim, et al., Energy benefit of the underfloor air distribution system for reducing air-conditioning and heating loads in buildings, *Indoor Built Environ.* 21 (1) (2012) 62–70.
- [18] S. Haghshenaskashani, B. Sajadi, M. Cehlin, Multi-objective optimization of impinging jet ventilation systems: Taguchi-based CFD method, *Build. Simulat.* 11 (6) (2018) 1207–1214.
- [19] X. Yang, X. Ye, B. Zuo, et al., Analysis of the factors influencing the airflow behavior in an impinging jet ventilation room, *Build. Simulat.* 14 (2021) 749–762.
- [20] Y. Wang, Z.A. Lian, Thermal comfort model for the non-uniform thermal environments, *Energy Build.* 172 (2018) 397–404.
- [21] Z. Lin, T.T. Chow, C.F. Tsang, et al., Stratum ventilation – a potential solution to elevated indoor temperatures, *Build. Environ.* 44 (11) (2009) 2256–2269.
- [22] Y. Cheng, Z. Lin, A.M. Fong, Effects of temperature and supply airflow rate on thermal comfort in a stratum-ventilated room, *Build. Environ.* 92 (2015) 269–277.
- [23] F. Cheng, S. Zhang, S. Gao, et al., Experimental investigation of airflow pattern and turbulence characteristics of stratum ventilation in heating mode, *Build. Environ.* 186 (2020) 107339.
- [24] S. Liang, B. Li, X. Tian, et al., Determining optimal parameter ranges of warm supply air for stratum ventilation using pareto-based MOPSO and cluster Analysis, *J. Build. Eng.* 37 (2021) 102145.
- [25] X. Kong, C. Xi, H. Li, et al., A comparative experimental study on the performance of mixing ventilation and stratum ventilation for space heating, *Build. Environ.* 157 (2019) 34–46.
- [26] S. Zhang, Z. Lin, Z. Ai, et al., Effects of operation parameters on performances of stratum ventilation for heating mode, *Build. Environ.* 148 (JAN) (2019) 55–66.
- [27] S. Zhang, Z. Lin, Z. Ai, et al., Multi-criteria performance optimization for operation of stratum ventilation under heating mode, *Appl. Energy* 239 (2019) 969–980.
- [28] American Society of Heating Refrigerating-And-Air-Conditioning-Engineers. ANSI/ASHRAE 55:2010 Thermal Environmental Conditions for Human Occupancy. 2010.
- [29] Y. Cheng, Z. Lin, Experimental investigation into the interaction between the human body and room Airflow and its effect on thermal comfort under stratum ventilation, *Indoor Air* 26 (2) (2016) 274–285.
- [30] Z. Lin, T. Yao, T. Chow, et al., Performance evaluation and design guidelines for stratum ventilation, *Build. Environ.* 46 (11) (2011) 2267–2279.
- [31] Q. Chen, Ventilation performance prediction for buildings: a method overview and recent applications, *Build. Environ.* 44 (4) (2008) 848–858.
- [32] A.Q. Ahmed, S. Gao, A.K. Kareem, A numerical study on the effects of exhaust locations on energy consumption and thermal environment in an office room served by displacement ventilation, *Energy Convers. Manag.* 117 (2016) 74–85.
- [33] Y. Zhou, Y. Deng, P. Wu, et al., The effects of ventilation and floor heating systems on the dispersion and deposition of fine particles in an enclosed environment, *Build. Environ.* 125 (2017) 192–205.
- [34] X. Shao, X. Li, X. Ma, et al., Long-term prediction of dynamic distribution of passive contaminant in complex recirculating ventilation system, *Build. Environ.* 121 (2017) 49–66.
- [35] K. Kosutova, T.V. Hooff, B. Blocken, CFD simulation of non-isothermal mixing ventilation in a generic enclosure: impact of computational and physical parameters, *Int. J. Therm. Sci.* 129 (2018) 343–357.
- [36] B. Rahmati, A. Heidarian, A.M. Jadidi, Investigation in performance of a hybrid under-floor air distribution with improved desk displacement ventilation system in a small office, *Appl. Therm. Eng.* 138 (2018) 861–872.
- [37] Fluent A (2013). Ansys Fluent Theory Guide. ANSYS Inc., USA, 15317(November), 724–746.
- [38] H. Per, Draught risk from cold vertical surfaces, *Pergamon* 29 (3) (1994) 297–301.
- [39] H. Manz, Analysis of thermal comfort near cold vertical surfaces by means of computational fluid dynamics, *Indoor Built Environ.* 13 (3) (2004) 233–242.
- [40] Y. Cheng, Z. Lin, Technical feasibility of a stratum-ventilated room for multiple rows of occupants, *Build. Environ.* 94 (2015) 580–592.
- [41] J. Deng, Control Problems of Grey Systems, vol. 1, North-holland, 1982, pp. 288–294, 5.
- [42] S. He, Y. Li, R. Wang, A new approach to performance analysis of ejector refrigeration system using grey system theory, *Appl. Therm. Eng.* 29 (8) (2008) 1592–1597.
- [43] S. Zhang, Y. Cheng, C. Huan, et al., Systematic comparisons of exit air temperature and wall temperature for modelling non-uniform thermal environment of stratum ventilation, *Build. Environ.* 149 (2019) 120–133.
- [44] Y. Ye, P. Xu, J. Mao, et al., Experimental Study on the Effectiveness of Internal Shading Devices, vol. 111, Elsevier, 2016, pp. 154–163.
- [45] C. Zhu, N. Li, D. Re, et al., Uncertainty in indoor air quality and grey system method, *Build. Environ.* 42 (4) (2006) 1711–1717.
- [46] S. Zhang, Y. Cheng, C. Huan, et al., Modeling non-uniform thermal environment of stratum ventilation with supply and exit air conditions, *Build. Environ.* 144 (2018) 542–554.
- [47] Y. Cheng, Z. Lin, Experimental study of airflow characteristics of stratum ventilation in a multi-occupant room with comparison to mixing ventilation and displacement ventilation, *Indoor Air* 25 (6) (2015) 662–671.